2021 60th IEEE Conference on Decision and Control (CDC)
December 13-15, 2021. Austin, Texas

Decentralized Optimal Merging Control for Connected and Automated Vehicles on Curved Roads

Wei Xiao and Christos G. Cassandras

Abstract— **This paper addresses the optimal control of Connected and Automated Vehicles (CAVs) arriving from two curved roads at a merging point where the objective is to jointly minimize the travel time, energy consumption, and passenger discomfort for each CAV. The solution guarantees that a speed-dependent safety constraint and a lateral rollover avoidance constraint are always satisfied, both at the merging point and everywhere within a control zone which precedes it. Our decentralized solution first determines the analytically tractable unconstrained optimal solution. We then use the previously developed joint Optimal Control and Barrier Function (OCBF) method to obtain a controller which optimally tracks such a solution while also guaranteeing all safety and control constraints. Simulation examples are included to compare the performance of the optimal controller to a baseline of human-driven vehicles with results showing significant improvements.**

I. INTRODUCTION

Traffic management at merging points (usually, highway on-ramps) is one of the most challenging problems within a transportation system in terms of safety, congestion, and energy consumption, in addition to being a source of stress for many drivers [1], [2], [3]. Advancements in next generation transportation system technologies and the emergence of CAVs have the potential to drastically improve a transportation network's performance by better assisting drivers in making decisions, ultimately reducing energy consumption, air pollution, congestion and accidents.

Centralized control mechanisms are normally used in forming platoons [4], [5], [6] in traffic control problems, where all vehicles in the same platoon can share the same control. This framework works when the safety constraints are independent of speed, and it is conservative for the merging problem as a vehicle may have to wait for a long time if there is a long platoon in the competing lane. Moreover, it is not easily amenable to disturbances.

A number of decentralized merging control mechanisms have been proposed [7], [8], [9], [10]. In this case, all computation is performed on board each vehicle and shared only with a small number of other vehicles which are affected by it. Optimal control problem formulations are used in some of these approaches, while Model Predictive Control (MPC) techniques are employed as an alternative, primarily to account for additional constraints and to compensate for disturbances by re-evaluating optimal actions [11], [12]. An alternative to MPC is provided in [13], [14] by the use of Control Barrier Functions (CBFs).

In our previous work [15], we developed a decentralized optimal control framework for each CAV approaching a merging point from one of two roads (often, a highway lane and an on-ramp lane). The objective combines minimizing (i) the travel time of each CAV over a given road segment from a point entering a Control Zone (CZ) to the eventual merging point and (ii) a measure of its energy consumption. However, this optimal control framework is computationally expensive, especially when one or more constraints become active. In order to improve the computational efficiency, we have developed a joint optimal control and barrier function (OCBF) framework in [13]. This framework can also consider model uncertainties, as well as process or measurement noise. We note that all the state of the art works mentioned above define the vehicle coordinates along its lane and do not consider the *curvature of the roads* that induces additional nonlinear safety constraints. Yet, we usually have curved roads in realistic traffic merging problems, especially in highway interchanges, in which case the centrifugal comfort and lateral rollover avoidance are also important.

In this paper, we address curved road merging problems where the cost is to jointly minimize travel time, energy consumption, as well as the centrifugal passenger discomfort. The safety constraints include maintaining a speed-dependent safe distance for collision avoidance at the merging point and everywhere within the CZ. The lateral rollover avoidance constraint is obtained through the Zero Moment Point (ZMP) [16] method that is usually used in balancing legged robots. We first derive the optimal solution when no constraints become active. Then, we employ the OCBF framework [13] to optimally track this solution while also guaranteeing the satisfaction of all constraints. Our OCBF framework allows us to study the tradeoff between travel time, centrifugal comfort and energy consumption. A simulation study of an actual curved road merging problem that arises in the Massachusetts Turnpike is included. The results show significant improvements in performance of the OCBF controller compared to a baseline with human-driven vehicles.

II. PROBLEM FORMULATION

The merging problem arises when traffic must be joined from two different roads, usually associated with a main lane and a merging lane as shown in Fig.1. We consider the case

This work was supported in part by NSF under grants ECCS-1931600, DMS-1664644, CNS-1645681, by AFOSR under grant FA9550-19-1-0158, by ARPA-E under grant DE-AR0001282 and by the NEXTCAR program under grant DEAR0000796, and by the MathWorks and by NPRP grant (12S-0228-190177) from the Qatar National Research Fund, a member of the Qatar Foundation (the statements made herein are solely the responsibility of the authors).

The authors are with the Division of Systems Engineering and Center for Information and Systems Engineering, Boston University, Brookline, MA, 02446, USA {xiaowei,cgc}@bu.edu

where all traffic consists of CAVs randomly arriving at the two curved lanes joined at the Merging Point (MP) M where a lateral collision may occur. The segment from the origin O or O' to the merging point M has a length L for both lanes and radii $r_{main} > 0, r_{merg} > 0$ for the main and merging lanes, respectively, and is called the Control Zone (CZ). All CAVs do not overtake each other in the CZ as each road consists of a single lane. A multi-lane merging problem has been studied in [17] (without road curvatures) and allows overtaking. Thus, the problem we consider in this paper can be extended to multi-lane cases along similar lines, in which case there are multiple MPs. A coordinator is associated with the MP whose function is to maintain a First-In-First-Out (FIFO) queue of CAVs based on their arrival time at the CZ and enable real-time communication with the CAVs that are in the CZ including the last one leaving the CZ. The FIFO assumption, imposed so that CAVs cross the MP in their order of arrival, is made for simplicity and often to ensure fairness, but can be relaxed through dynamic resequencing schemes [18]. An explicit resequencing method is included in Section IV.D of this paper.

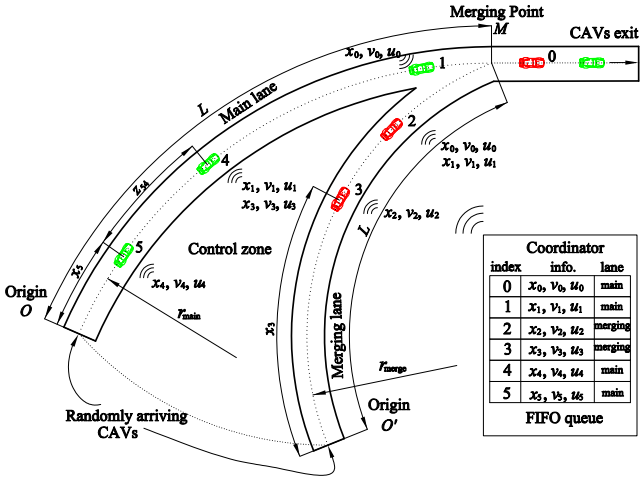

Fig. 1. The merging problem for roads with curvature

Let $S(t)$ be the set of FIFO-ordered (acccording to arrival times at O or O') indices of all CAVs located in the CZ at time t along with the CAV (whose index is 0 as shown in Fig.1) that has just left the CZ. Let $N(t)$ be the cardinality of $S(t)$. Thus, if a CAV arrives at O or O' at time t, it is assigned the index $N(t)$. All CAV indices in $S(t)$ decrease by one when a CAV passes over the MP and the vehicle whose index is -1 is dropped.

The vehicle dynamics for each CAV $i \in S(t)$ along the lane to which it belongs take the form

$$\dot{x}_i(t) = v_i(t), \qquad \dot{v}_i(t) = u_i(t), \tag{1}$$

where $x_i(t)$ denotes the distance to the origin O (O') along the main (merging) lane if the vehicle i is located in the main (merging) lane, $v_i(t)$ denotes the velocity, and $u_i(t)$ denotes the control input (acceleration). We consider three objectives for each CAV subject to four constraints, as detailed next.

Objective 1 (Minimizing travel time): Let t_i^0 and t_i^m denote the time that CAV $i \in S(t)$ arrives at the origin O or O' and the merging point M, respectively. We wish to minimize the travel time $t_i^m - t_i^0$ for CAV i.

Objective 2 (Minimizing energy consumption): We also wish to minimize energy consumption for each $i \in S(t)$:

$$\min_{u_i(t)} \int_{t_i^0}^{t_i^m} C_i(u_i(t))dt, \tag{2}$$

where $C_i(\cdot)$ is a strictly increasing function of its argument, and it usually takes the quadratic form: $C_i(u_i(t)) = u_i^2(t)$.

Objective 3 (Maximizing centrifugal comfort): In order to minimize the centrifugal discomfort (or maximize the comfort), we wish to minimize the centrifugal acceleration

$$\min_{u_i(t)} \int_{t_i^0}^{t_i^m} \kappa(x_i(t))v_i^2(t)dt, \tag{3}$$

where $\kappa : \mathbb{R} \to \mathbb{R}^{\geq 0}$ is the curvature of the road at position x_i. The curvature $\kappa(x_i)$ has a sign, and is determined by $\frac{1}{r(x_i)}$, where $r : \mathbb{R} \to \mathbb{R}$ is the radius of the road at x_i. Since we just wish to minimize the centrifugal acceleration, we ignore the sign and set $\kappa(x_i) \geq 0$ in this paper.

Constraint 1 (Safety constraints): Let i_p denote the index of the CAV which physically immediately precedes i in the CZ (if one is present). We require that the distance $z_{i,i_p}(t) := x_{i_p}(t) - x_i(t)$ be constrained by the speed $v_i(t)$ of CAV $i \in S(t)$ so that

$$z_{i,i_p}(t) \geq \varphi v_i(t) + \delta, \quad \forall t \in [t_i^0, t_i^m], \tag{4}$$

where φ denotes the reaction time (as a rule, $\varphi = 1.8$ is used, e.g., [19]). If we define z_{i,i_p} to be the distance from the center of CAV i to the center of CAV i_p, then δ is a constant determined by the length of these two CAVs (taken to be a constant over all CAVs for simplicity).

Constraint 2 (Safe merging): There should be enough safe space at the MP M for a CAV (which eventually becomes CAV 1, as shown in Fig. 1) to cut in, i.e.,

$$z_{1,0}(t_1^m) \geq \varphi v_1(t_1^m) + \delta. \tag{5}$$

Constraint 3 (Vehicle limitations): There are constraints on the speed and acceleration for each $i \in S(t)$:

$$\begin{aligned} v_{i,min} \leq v_i(t) \leq v_{i,max}, \quad \forall t \in [t_i^0, t_i^m], \\ u_{min} \leq u_i(t) \leq u_{max}, \quad \forall t \in [t_i^0, t_i^m], \end{aligned} \tag{6}$$

where $v_{i,max} > 0$ and $v_{i,min} \geq 0$ denote the maximum and minimum speed allowed in the CZ, while $u_{min} < 0$ and $u_{max} > 0$ denote the minimum and maximum control, respectively.

Constraint 4 (Lateral safety constraint): Finally, there is a constraint on the centrifugal acceleration to avoid lateral rollover for each $i \in S(t)$:

$$\kappa(x_i(t))v_i^2(t) \leq \frac{w_i^h}{h_i} g, \quad \forall t \in [t_i^0, t_i^m], \tag{7}$$

where $w_i^h > 0$ denotes the half-width of the vehicle, $h_i > 0$ denotes the height of the center of gravity with respect to

the ground, and g is the gravity constant. The above lateral safety constraint is obtained through the Zero Moment Point (ZMP) [16] method (assuming the road lateral slope is zero) that balances the CAV considering both gravity and inertia.

Problem Formulation. Our goal is to determine a control law to achieve objectives 1-3 subject to constraints 1-4 for each $i \in S(t)$ governed by the dynamics (1). We first choose $C_i(u_i(t)) = \frac{1}{2}u_i^2(t)$ in (2), noting that the OCBF method allows for more elaborate fuel consumption models, e.g., as in [20]; we shall limit ourselves to this model in this paper. Normalizing each objective, and combining objectives 1, 2 and 3 with $\alpha_1 \in [0,1], \alpha_2 \in [0, 1-\alpha_1]$, we formulate the following optimal control problem for each CAV:

$$\min_{u_i(t)} \int_{t_i^0}^{t_i^m} \left[\alpha_1 + \alpha_2 \frac{\kappa(x_i(t))v_i^2(t)}{\kappa_{\max} v_{\max}^2} + (1-\alpha_1-\alpha_2)\frac{\frac{1}{2}u_i^2(t)}{\frac{1}{2}u_{\lim}^2}\right] dt, \tag{8}$$

subject to (1), (4), (5), (6), (7), the initial and terminal position conditions $x_i(t_i^0) = 0$, $x_i(t_i^m) = L$, and given t_i^0, v_i^0 (where v_i^0 denotes the initial speed). $u_{\lim} = \max\{u_{\max}^2, u_{\min}^2\}$. The weight factor $\alpha_1 \geq 0, \alpha_2 \geq 0$ can be adjusted to penalize travel time and comfort relative to the energy cost.

Multiplying (8) by $\frac{u_{\lim}^2}{2(1-\alpha_1-\alpha_2)}$ and letting $\beta_1 = \frac{\alpha_1 u_{\lim}^2}{2(1-\alpha_1-\alpha_2)}$ and $\beta_2 = \frac{\alpha_2 u_{\lim}^2}{2(1-\alpha_1-\alpha_2)\kappa_{\max} v_{\max}^2}$, we have a simplified and normalized version of (8):

$$\min_{u_i(t)} \int_{t_i^0}^{t_i^m} \left[\beta_1 + \beta_2 \kappa(x_i(t))v_i^2(t) + \frac{1}{2}u_i^2(t)\right] dt. \tag{9}$$

III. DECENTRALIZED ONLINE FRAMEWORK

Note that (9) can be locally solved by each CAV i provided that there is some information sharing with two other CAVs: CAV i_p which physically immediately precedes i and is needed in (4) and CAV $i-1$ so that i can determine whether this CAV is located in the same lane or not. With this information, CAV i can determine which of two possible cases applies: (i) $i_p = i-1$, i.e., i_p is the CAV immediately preceding i in the FIFO queue (e.g., $i = 3, i_p = 2$ in Fig. 1), and (ii) $i_p < i-1$, which implies that CAV $i-1$ is in a different lane from i (e.g., $i = 4, i_p = 1, i-1 = 3$ in Fig. 1). It is now clear that we can solve problem (9) for any $i \in S(t)$ in a decentralized way in the sense that CAV i needs only its own local state information and state information from $i-1$, as well as from i_p in case (ii). Observe that if $i_p = i-1$, then (5) is a redundant constraint; otherwise, we need to separately consider (4) and (5). Therefore, we will analyze each of these two cases in what follows.

Assumption 1: The safety constraint (4), state constraints (6), and lateral safety constraint (7) are not active at t_i^0.

Since CAVs arrive randomly, we can handle violations of Assumption 1 by foregoing optimality and simply controlling a CAV that violates Assumption 1 until all constraints become feasible within the CZ using the CBF method [13].

Under Assumption 1, we will start by analyzing the case of no active constraints. The analysis of the cases where one or more constraints become active is similar to [15]. However, the computational time significantly increases with constrained optimal solutions, which prevents the optimal control from being implementable in real-world merging problems. Therefore, in this paper, we use CBFs [21] [22] to guarantee the satisfaction of all the constraints, and employ the OCBF framework [13] to optimally track the tractable unconstrained optimal solutions.

A. Unconstrained Optimal Control

Let $\mathcal{X}_i(t) := (x_i(t), v_i(t))$ be the state vector and $\boldsymbol{\lambda}_i(t) := (\lambda_i^x(t), \lambda_i^v(t))$ be the costate vector (for simplicity, in the sequel we omit explicit time dependence when no ambiguity arises). The Hamiltonian with the state constraint, control constraint and safety constraint adjoined is

$$\begin{aligned} H_i(\mathcal{X}_i, \boldsymbol{\lambda}_i, u_i) =& \frac{1}{2}u_i^2 + \beta_2\kappa(x_i)v_i^2 + \lambda_i^x v_i + \lambda_i^v u_i \\ &+ \mu_i^a(u_i - u_{max}) + \mu_i^b(u_{min} - u_i) \\ &+ \mu_i^c(v_i - v_{max}) + \mu_i^d(v_{min} - v_i) \\ &+ \mu_i^e(x_i + \varphi v_i + \delta - x_{i_p}) \\ &+ \mu_i^f(\kappa(x_i)v_i^2 - \frac{w_i^h}{h_i}g) + \beta_1. \end{aligned} \tag{10}$$

The Lagrange multipliers $\mu_i^a, \mu_i^b, \mu_i^c, \mu_i^d, \mu_i^e, \mu_i^f$ are positive when the constraints are active and become 0 when the constraints are strict. Note that when the safety constraint (4) becomes active, i.e., $\mu_i^e > 0$, the expression above involves $x_{i_p}(t)$. When $i = 1$, the optimal trajectory is obtained without this term, since (4) is inactive over all $[t_1^0, t_1^m]$. Thus, once the solution for $i = 1$ is obtained (based on the analysis that follows), x_1^* is a given function of time and available to $i = 2$. Based on this information, the optimal trajectory of $i = 2$ is obtained. Similarly, all subsequent optimal trajectories for $i > 2$ can be recursively obtained based on $x_{i_p}^*(t)$ with $i_p = i-1$.

Since the terminal state constraint $\psi_{i,1} := x_i(t_i^m) - L = 0$ is not an explicit function of time, the transversality condition [23] is

$$H_i(\mathcal{X}_i(t), \boldsymbol{\lambda}_i(t), u_i(t))|_{t=t_i^m} = 0, \tag{11}$$

with the costate boundary condition $\boldsymbol{\lambda}_i(t_i^m) = [(\nu_{i,1}\frac{\partial \psi_{i,1}}{\partial \mathcal{X}_i})^T]_{t=t_i^m}$, where $\nu_{i,1}$ denotes a Lagrange multiplier.

The Euler-Lagrange equations become

$$\dot{\lambda}_i^x = -\frac{\partial H_i}{\partial x_i} = -\mu_i^e - \beta_2 \frac{\partial \kappa(x_i)}{\partial x_i}v_i^2 - \mu_i^f \frac{\partial \kappa(x_i)}{\partial x_i}v_i^2, \tag{12}$$

and

$$\begin{aligned} \dot{\lambda}_i^v &= -\frac{\partial H_i}{\partial v_i} \\ &= -\lambda_i^x - \mu_i^c + \mu_i^d - \varphi\mu_i^e - 2\beta_2\kappa(x_i)v_i - 2\mu_i^f\kappa(x_i)v_i, \end{aligned} \tag{13}$$

and the necessary condition for optimality is

$$\frac{\partial H_i}{\partial u_i} = u_i + \lambda_i^v + \mu_i^a - \mu_i^b = 0. \tag{14}$$

Since the curvature $\kappa(x_i)$ of the road usually depends on the specific road configuration and it prevents the derivation of an explicit solution, we replace $\kappa(x_i)$ by the average (or

possibly maximum) curvature $\hat{\kappa} \geq 0$ of the road in the CZ. In the case of no active constraints throughout an optimal trajectory, we also have $\mu_i^a = \mu_i^b = \mu_i^c = \mu_i^d = \mu_i^e = \mu_i^f = 0$. Applying (14), the optimal control input is given by $u_i + \lambda_i^v = 0$. and the Euler-Lagrange equation (13) yields $\dot{\lambda}_i^v = -\lambda_i^x - 2\beta_2\hat{\kappa}v_i$. In the case of no active constraints throughout an optimal trajectory, (12) implies $\lambda_i^x(t) = a_i$, where a_i is an integration constant. Combining the last two equations, we have $\dot{u}_i = a + 2\beta_2\hat{\kappa}v_i$.

Combining dynamics (1) with the above, we have

$$\ddot{v}_i = a + 2\beta_2\hat{\kappa}v_i. \tag{15}$$

We can solve this differential equation and get the explicit solution for the speed as

$$v_i^*(t) = b_i e^{\sqrt{2\beta_2\hat{\kappa}}t} + c_i e^{-\sqrt{2\beta_2\hat{\kappa}}t} - \frac{a_i}{2\beta_2\hat{\kappa}}, \tag{16}$$

where b_i, c_i are integration constants.

Consequently, we obtain the following optimal solution for the unconstrained problem:

$$u_i^*(t) = \sqrt{2\beta_2\hat{\kappa}}(b_i e^{\sqrt{2\beta_2\hat{\kappa}}t} - c_i e^{-\sqrt{2\beta_2\hat{\kappa}}t}), \tag{17}$$

$$x_i^*(t) = \frac{1}{\sqrt{2\beta_2\hat{\kappa}}}(b_i e^{\sqrt{2\beta_2\hat{\kappa}}t} - c_i e^{-\sqrt{2\beta_2\hat{\kappa}}t}) - \frac{a_i}{2\beta_2\hat{\kappa}}t + d_i, \tag{18}$$

where d_i is also an integration constant. In addition, we have the initial conditions $x_i(t_i^0) = 0, v_i(t_i^0) = v_i^0$ and the terminal condition $x_i(t_i^m) = L$. The costate boundary conditions and (14) offer us $u_i(t_i^m) = -\lambda_i^v(t_i^m) = 0$ and $\boldsymbol{\lambda}_i(t_i^m) = (a_i, 0)$, therefore, the transversality condition (11) gives us an additional relationship:

$$\beta_1 + \beta_2\hat{\kappa}v_i^2(t_i^m) + a_i v_i(t_i^m) = 0. \tag{19}$$

Then, for each $i \in S(t)$, we need to solve the following five nonlinear algebraic equations to get a_i, b_i, c_i, d_i and t_i^m:

$$\begin{aligned}
&b_i e^{\sqrt{2\beta_2\hat{\kappa}}t_i^0} + c_i e^{-\sqrt{2\beta_2\hat{\kappa}}t_i^0} - \frac{a_i}{2\beta_2\hat{\kappa}} = v_i^0,\\
&\frac{1}{\sqrt{2\beta_2\hat{\kappa}}}(b_i e^{\sqrt{2\beta_2\hat{\kappa}}t_i^0} - c_i e^{-\sqrt{2\beta_2\hat{\kappa}}t_i^0}) - \frac{a_i}{2\beta_2\hat{\kappa}}t_i^0 + d_i = 0,\\
&\frac{1}{\sqrt{2\beta_2\hat{\kappa}}}(b_i e^{\sqrt{2\beta_2\hat{\kappa}}t_i^m} - c_i e^{-\sqrt{2\beta_2\hat{\kappa}}t_i^m}) - \frac{a_i}{2\beta_2\hat{\kappa}}t_i^m + d_i = L,\\
&\sqrt{2\beta_2\hat{\kappa}}(b_i e^{\sqrt{2\beta_2\hat{\kappa}}t_i^m} - c_i e^{-\sqrt{2\beta_2\hat{\kappa}}t_i^m}) = 0,\\
&\beta_1 + \beta_2\hat{\kappa}(b_i e^{\sqrt{2\beta_2\hat{\kappa}}t_i^m} + c_i e^{-\sqrt{2\beta_2\hat{\kappa}}t_i^m} - \frac{a_i}{2\beta_2\hat{\kappa}})^2\\
&\qquad + a_i(b_i e^{\sqrt{2\beta_2\hat{\kappa}}t_i^m} + c_i e^{-\sqrt{2\beta_2\hat{\kappa}}t_i^m} - \frac{a_i}{2\beta_2\hat{\kappa}}) = 0.
\end{aligned} \tag{20}$$

Note that when $\beta_2 \to 0$ (i.e., $\alpha_2 \to 0$), the optimal control (17) degenerates to the case without any comfort consideration. In other words, the optimal control (17) is in linear form as in [15]: $\lim_{\beta_2 \to 0} u_i(t) = f_a t + f_b$, where $f_a = 2\beta_2\hat{\kappa}(b_i + c_i), f_b = \sqrt{2\beta_2\hat{\kappa}}(b_i - c_i)$ following a Taylor series expansion.

The equations in (20) are usually hard to solve as there are too many exponential terms (it usually takes about one second using *solve* in Matlab to solve them). This motivates us to use a computationally efficient solution approach as shown in the next subsection.

B. Explicit Solution for Integration Constants

In this section, we show how to determine an explicit solution for the integration constants of the optimal control (17) which significantly reduces the computational complexity. By Lemma 2 in [15], we have $t_i^m - t_i^0 = t_j^m - t_j^0$ if $v_i^0 = v_j^0, i \in S(t), j \in S(t)$ if $\beta_2 = 0$. This is also true if $\beta_2 > 0$ as the total travel time clearly does not depend on the arrival time t_i^0 of a CAV $i \in S(t)$. Moreover, observe that v_i^0 shows up only in the first of the five equations in (20). Therefore, given β_1, β_2, we can get the solution for t_i^m for some fixed $v_i^0 \in [v_{min}, v_{max}]$ by solving (20) off line with $t_i^0 = 0$. We can then construct a look-up table over a finite number of v_i^0 values constrained by $v_i^0 \in [v_{min}, v_{max}]$ and use a simple linear interpolation for any possible v_i^0 value actually observed. However, since v_i^0 is continuous and this approach may induce non-negligible errors, we choose instead to use regression (e.g., with polynomial or Gaussian kernels) to obtain the solution of t_i^m for all $v_i^0 \in [v_{min}, v_{max}]$ in the form:

$$t_i^m = t_i^0 + R(v_i^0), \tag{21}$$

where $R : \mathbb{R} \to \mathbb{R}$ denotes the regression model. Thus, we can immediately obtain t_i^m on line from (21) for any CAV arriving at time t_i^0 with speed v_i^0.

Since the last equation of (20) is used to determine t_i^m which is already evaluated as discussed above, it remains to use the first four equations to determine a_i, b_i, c_i, d_i, which are all in linear form. Therefore, we can get

$$\begin{bmatrix} a_i \\ b_i \\ c_i \\ d_i \end{bmatrix} = \begin{bmatrix} -\frac{1}{2\beta_2\hat{\kappa}} & e^{\sqrt{2\beta_2\hat{\kappa}}t_i^0} & e^{-\sqrt{2\beta_2\hat{\kappa}}t_i^0} & 0 \\ -\frac{t_i^0}{2\beta_2\hat{\kappa}} & \frac{e^{\sqrt{2\beta_2\hat{\kappa}}t_i^0}}{\sqrt{2\beta_2\hat{\kappa}}} & -\frac{e^{-\sqrt{2\beta_2\hat{\kappa}}t_i^0}}{\sqrt{2\beta_2\hat{\kappa}}} & 1 \\ -\frac{t_i^m}{2\beta_2\hat{\kappa}} & \frac{e^{\sqrt{2\beta_2\hat{\kappa}}t_i^m}}{\sqrt{2\beta_2\hat{\kappa}}} & -\frac{e^{-\sqrt{2\beta_2\hat{\kappa}}t_i^m}}{\sqrt{2\beta_2\hat{\kappa}}} & 1 \\ 0 & e^{\sqrt{2\beta_2\hat{\kappa}}t_i^m} & -e^{-\sqrt{2\beta_2\hat{\kappa}}t_i^m} & 0 \end{bmatrix}^{-1} \begin{bmatrix} v_i^0 \\ 0 \\ L \\ 0 \end{bmatrix}, \tag{22}$$

The above equation is then the explicit solution for the four integration constants of (17), and it is much more computationally efficient than solving (20). The above matrix is invertible if there exists a solution in (20).

C. Constrained Optimal Control

When one or more constraints in the merging problem becomes active, we can use the interior point analysis [23] to find the complete constrained optimal control solution, similar to the comfort-free case shown in [15]. However, the solution can become complicated when two or more constraints become active in an optimal trajectory, which makes the solution time-consuming to obtain, hence possibly prohibitive for real-time implementation. It is for this reason that we resort to the CBF method to guarantee the satisfaction of all constraints while sacrificing some performance if some constraints become active. This method can be implemented on line for merging problems as detailed in [13].

D. Joint Optimal Control and Barrier Function (OCBF)

In this section, we briefly review the OCBF approach in [13] as it applies to our problem. The OCBF controller aims to track the OC solution (17)-(18) while satisfying all

constraints (4), (6) and (5). Each of the constraints in (4), (6), (7) and (5) can be enforced by a CBF. In the CBF approach, each of the continuously differentiable *state* constraints is mapped onto another constraint on the *control* input such that the satisfaction of this new constraint implies the satisfaction of the original constraint [21], [22]. In addition, a Control Lyapunov Function (CLF) [21] can also be used to track (stabilize) the optimal speed trajectory (16)

Therefore, the OCBF controller solves the following:

$$\min_{u_i(t),e_i(t)} J_i(u_i(t),e_i(t))=\int_{t_i^0}^{t_i^m}\left(\beta e_i^2(t)+\frac{1}{2}(u_i(t)-u_{ref}(t))^2\right)dt, \tag{23}$$

subject to the CBF constraints that enforce (4), (6), (7) and (5), and the CLF constraint for tracking, where $\beta > 0$ and $e_i(t)$ is a relaxation variable in the CLF constraint. The obvious selection for acceleration reference signal is $u_{ref}(t) = u_i^*(t)$ given by (17). However, we can improve the tracking process using $x_i^*(t)$ from (18) and selecting instead: $u_{ref}(t) = \frac{x_i^*(t)}{x_i(t)}u_i^*(t)$. Alternative choices of $u_{ref}(t)$ are also possible as shown in [14], [13].

We refer to the resulting control $u_i(t)$ in (23) as the OCBF control. The solution to (23) is obtained by discretizing the time $[t_i^0, t_i^m]$ with time steps of length Δ and solving (23) over $[t_i^0+k\Delta, t_i^0+(k+1)\Delta]$, $k = 0, 1, \ldots$, with $u_i(t), e_i(t)$ as decision variables held constant over each such interval. Consequently, each such problem is a QP since we have a quadratic cost and a number of linear constraints on the decision variables at the beginning of each interval. The solution of each such problem gives $u_i^*(t_i^0 + k\Delta)$, $k = 0, 1, \ldots$, allowing us to update (1) in the k^{th} time interval. This process is repeated until CAV i leaves the CZ.

E. Dynamic Resequencing

The FIFO assumption imposed on the curved-road merging problem can potentially decrease CAV performance as the main and merging roads may have different curvatures. This non-symmetric structure generally benefits from non-FIFO CAV ordering as observed in [18]. In order to relax the FIFO assumption, the Optimal Dynamic Resequencing (ODR) approach in [18] includes a step before a new CAV arrives at one of the origins where the CAV obtains the constrained optimal solution and uses the joint objective function to determine the passing order at the MP. This approach is computationally expensive and, as already seen, the constrained optimal solutions are harder to be found in the curved-road merging problem.

In order to improve the computational efficiency of this process, we will relax the requirement for *optimal* resequencing by considering only the travel time under the unconstrained optimal control (17) as the objective used to determine the passing order. Since this resequencing may not be the optimal policy, we refer to it as Dynamic Resequencing (DR). Specifically, if the MP arrival time t_i^m under the unconstrained optimal control (17) of a new arrival CAV $i \in S(t)$ satisfies

$$t_j^m - t_i^m \geq \varphi + \frac{\delta}{v_j^*(t_i^m)}, \tag{24}$$

for some $j \in S(t)$ such that $i_p < j < i$ (i.e., j is located at the other lane from i), then the new arrival CAV i overtakes CAV j under $v_j^*(t_i^m)$ which is the unconstrained optimal speed of j from (16) at time t_i^m. If such j is found in (24), its safe merging constraint will change after resequencing. We need to deal with the possible infeasibility problem of the QP, and this will be further studied.

IV. SIMULATION EXAMPLES

We have used the Vissim microscopic multi-model traffic flow simulation tool as a baseline to compare with the optimal control approach we have developed. The car following model in Vissim is based on [24] and simulates human psycho-physiological driving behavior.

We choose a merging scenario of highway I-90 (known as the Massachusetts Turnpike), in the Boston area in the USA, as shown in Fig. 2. All CAVs start to communicate with a coordinator (at the merging point) in the resequencing/connection zone as shown in the figure.

Fig. 2. A merging scenario of the I-90 Masschussets Turnpike, USA.

The parameters of the map are as follows: $L = 200m$, $\hat{\kappa} = \frac{1}{200}, v_{i,max} = 20m/s$ in the main lane, and $\hat{\kappa} = \frac{1}{50}, v_{i,max} = 15m/s$ in the merging lane. $\Delta = 0.1s, \varphi = 1.8s, \delta = 0m, v_{min} = 0m/s, u_{max} = -u_{min} = 0.4g, g = 9.81m/s^2$. We set different cost weights for the main and merging roads, i.e., we set $\alpha_1 = 0.3, \alpha_2 = 0.1$ in the main lane, and $\alpha_1 = 0.3, \alpha_2 = 0.4$ in the merging lane. The simulation under optimal control is conducted in MATLAB by using the same arrival process input and initial conditions as in Vissim. The CAVs enter the CZ under a Poisson arrival process with an initial speed in the range $6.5-12.5m/s$ at the origins. The MATLAB computation time for the proposed framework is very efficient, i.e., less than $0.01s$ for each QP of the OCBF controller (23) (Intel(R) Core(TM) i7-8700 CPU @ 3.2GHz×2).

The simulation results of optimal control under two traffic densities compared to that in Vissim are summarized in Table I. Since we choose different α_1, α_2 for the main and merging lanes, we list the metrics separately in Table I.

When the traffic rates in the main and merging lanes are equal at 500 CAVs/h, the overall objective function of CAVs

TABLE I

OBJECTIVE FUNCTION COMPARISON

Rate(CAVs/h)	Main:500, Merg.:500			Main:500, Merg.:800		
Method	Vissim	OCBF	DR	Vissim	OCBF	DR
Main time (s)	22.27	13.35	12.49	22.43	15.57	13.30
Main comfort	9.07	15.75	16.71	9.03	13.46	15.72
Main $\frac{1}{2}u_i^2(t)$	1.21	10.93	10.42	1.23	12.86	14.35
Main obj.	92.76	72.42	69.22	93.37	81.43	75.63
Merg. time (s)	26.71	15.92	15.94	39.02	16.40	16.32
Merg. comfort	35.89	50.77	50.73	30.61	49.50	49.75
Merg. $\frac{1}{2}u_i^2(t)$	13.78	0.05	1.13	13.29	1.79	3.20
Merg. obj.	301.3	238.4	239.6	606.6	241.0	242.3

in the main road improves about 22% with the OCBF method (using FIFO) compared with Vissim, and it further improves about 4% with the OCBF method when DR is included. Note that the energy consumption in the main lane is 10 times worse for the OCBF method relative to Vissim, while the energy consumption in the merging lane is 10 times better for the OCBF method. This is due to the fact that the CAVs in the main lane have a higher speed limit than the ones in the merging lane. Therefore, a CAV i in the main lane may use a large energy consumption in order to satisfy the safe merging constraint at the MP when it has to coordinate with a CAV $i-1$ whose speed is low in the merging lane. We have similar results when the arrival rate increases to 800 CAVs/h in the merging lane.

When traffic arrival rate increases to 1000 CAVs/h for both the main and merging lanes, the human driven vehicles of the merging lane will cause heavy traffic congestion in Vissim, while the OCBF method can successfully manage the traffic without any congestion (see videos[1]).

V. CONCLUSIONS

We have derived a decentralized optimal control framework for the curved road traffic merging problem that jointly minimizes the travel time and energy consumption, as well as the centrifugal discomfort of each CAV and guarantees that a speed-dependent safety constraint and a lateral rollover avoidance constraint are always satisfied. Ongoing research is extending the proposed framework to multi-lane cases, using better energy models and CAV dynamics, and most importantly, exploring the feasibility guarantee of the proposed framework under tight control bounds.

REFERENCES

[1] B. Schrank, B. Eisele, T. Lomax, and J. Bak. (2015) The 2015 urban mobility scorecard. Texas A&M Transportation Institute. [Online]. Available: http://mobility.tamu.edu

[2] M. Tideman, M. van der Voort, B. van Arem, and F. Tillema, "A review of lateral driver support systems," in *Proc. IEEE Intelligent Transportation Systems Conference*, pp. 992–999, Seatle, 2007.

[3] D. D. Waard, C. Dijksterhuis, and K. A. Broohuis, "Merging into heavy motorway traffic by young and elderly drivers," *Accident Analysis and Prevention*, vol. 41, no. 3, pp. 588–597, 2009.

[1] https://sites.google.com/view/xiaowei2021/research?authuser=0#h.o3pn0s7rv2ye

[4] S. E. Shladover, C. A. Desoer, J. K. Hedrick, M. Tomizuka, J. Walrand, W.-B. Zhang, D. H. McMahon, H. Peng, S. Sheikholeslam, and N. McKeown, "Automated vehicle control developments in the path program," *IEEE Transactions on Vehicular Technology*, vol. 40, no. 1, pp. 114–130, 1991.

[5] R. Rajamani, H.-S. Tan, B. K. Law, and W.-B. Zhang, "Demonstration of integrated longitudinal and lateral control for the operation of automated vehicles in platoons," *IEEE Transactions on Control Systems Technology*, vol. 8, no. 4, pp. 695–708, 2000.

[6] H. Xu, S. Feng, Y. Zhang, and L. Li, "A grouping-based cooperative driving strategy for cavs merging problems," *IEEE Transactions on Vehicular Technology*, vol. 68, no. 6, pp. 6125–6136, 2019.

[7] V. Milanes, J. Godoy, J. Villagra, and J. Perez, "Automated on-ramp merging system for congested traffic situations," *IEEE Transactions on Intelligent Transportation Systems*, vol. 12, no. 2, pp. 500–508, 2012.

[8] G. Raravi, V. Shingde, K. Ramamritham, and J. Bharadia, *Merge algorithms for intelligent vehicles. In: Sampath, P, Ramesh, S. (Eds.), Next Generation Design and Verification Methodologies for Distributed Embedded Control Systems*. Waltham, MA: Springer, 2007.

[9] R. Scarinci and B. Heydecker, "Control concepts for facilitating motorway on-ramp merging using intelligent vehicles," *Transport Reviews*, vol. 34, no. 6, pp. 775–797, 2014.

[10] Y. Bichiou and H. A. Rakha, "Developing an optimal intersection control system for automated connected vehicles," *IEEE Transactions on Intelligent Transportation Systems*, vol. 20, no. 5, pp. 1908–1916, 2019.

[11] M. Mukai, H. Natori, and M. Fujita, "Model predictive control with a mixed integer programming for merging path generation on motor way," in *Proc. IEEE Conference on Control Technology and Applications*, pp. 2214–2219, Mauna Lani, 2017.

[12] M. H. B. M. Nor and T. Namerikawa, "Merging of connected and automated vehicles at roundabout using model predictive control," in *Annual Conference of the Society of Instrument and Control Engineers of Japan*, pp. 272–277, 2018.

[13] W. Xiao, C. G. Cassandras, and C. Belta, "Bridging the gap between optimal trajectory planning and safety-critical control with applications to autonomous vehicles," *Automatica*, vol. 129, p. 109592, 2021.

[14] ——, "Decentralized merging control in traffic networks with noisy vehicle dynamics: A joint optimal control and barrier function approach," in *Proc. IEEE 22nd Intelligent Transportation Systems Conference*, 2019, pp. 3162–3167.

[15] W. Xiao and C. G. Cassandras, "Decentralized optimal merging control for connected and automated vehicles with safety constraint guarantees," *Automatica*, vol. 123.109333, 2021.

[16] P. Sardain and G. Bessonnet, "Forces acting on a biped robot. center of pressure-zero moment point," *IEEE Transactions on Systems, Man, and Cybernetics - Part A: Systems and Humans*, vol. 34, no. 5, pp. 630–637, 2004.

[17] W. Xiao, C. G. Cassandras, and C. Belta, "Decentralized optimal control in multi-lane merging for connected and automated vehicles," in *Proc. IEEE 23nd Intelligent Transportation Systems Conference*, 2020, pp. 1–6.

[18] W. Xiao and C. G. Cassandras, "Decentralized optimal merging control for connected and automated vehicles with optimal dynamic resequencing," in *Proc. of the American Control Conference*, 2020, pp. 4090–4095.

[19] K. Vogel, "A comparison of headway and time to collision as safety indicators," *Accident Analysis & Prevention*, vol. 35, no. 3, pp. 427–433, 2003.

[20] M. Kamal, M. Mukai, J. Murata, and T. Kawabe, "Model predictive control of vehicles on urban roads for improved fuel economy," *IEEE Transactions on Control Systems Technology*, vol. 21, no. 3, pp. 831–841, 2013.

[21] A. D. Ames, S. Coogan, M. Egerstedt, G. Notomista, K. Sreenath, and P. Tabuada, "Control barrier functions: Theory and applications," in *Proc. of the European Control Conference*, 2019, pp. 3420–3431.

[22] W. Xiao and C. Belta, "Control barrier functions for systems with high relative degree," in *Proc. of 58th IEEE Conference on Decision and Control*, Nice, France, 2019, pp. 474–479.

[23] Bryson and Ho, *Applied Optimal Control*. Waltham, MA: Ginn Blaisdell, 1969.

[24] R. Wiedemann, "Simulation des straenverkehrsflusses," in *Proc. of the Schriftenreihe des tnstituts fir Verkehrswesen der Universitiit Karlsruhe (In German language)*, 1974.